Journal of Biomedical Optics

SPIEDigitalLibrary.org/jbo

Fluorescence spectroscopy as a highly potential single-entity tool to identify chromophores and fluorophores: study on neoplastic human brain lesions

Shaiju S. Nazeer
Ariya Saraswathy
Arun Kumar Gupta
Ramapurath S. Jayasree

SPIE

Fluorescence spectroscopy as a highly potential single-entity tool to identify chromophores and fluorophores: study on neoplastic human brain lesions

Shaiju S. Nazeer,[a] Ariya Saraswathy,[a] Arun Kumar Gupta,[b] and Ramapurath S. Jayasree[a]
[a]Sree Chitra Tirunal Institute for Medical Sciences and Technology, Biophotonics and Imaging Lab, Biomedical Technology Wing, Poojappura, Thiruvananthapuram, Kerala, 695 012, India
[b]National Institute of Mental Health and Neuro Sciences, Department of Neuroimaging and Interventional Radiology, Bangalore, Karnataka, 560029, India

Abstract. Fluorescence and diffuse reflectance spectroscopy are powerful tools to differentiate normal and malignant tissue based on the emissions from endogenous fluorophores and diffuse reflection of absorbers such as hemoglobin. However, separate analytical methods are used for the identification of fluorophores and hemoglobin. The estimation of fluorophores and hemoglobin simultaneously using a single technique of autofluorescence spectroscopy is reported, and its diagnostic potential on clinical tissue samples is potentially exploited. Surgically removed brain tissues from patients that are later identified pathologically as astrocytoma, glioma, meningioma, and schwannoma are studied. The emissions from prominent fluorophores collagen, flavin adenine dinucleotide, phospholipids, and porphyrin are analyzed at 320 and 410 nm excitations. The hemoglobin concentration is also calculated from the ratio of fluorescence emissions at 500 and 570 nm. A better classification of normal and tumor tissues is yielded for 410 nm excitation compared to 320 nm when diagnostic algorithm based on linear discriminant analysis is used. The potential of fluorescence spectroscopy as a single entity to evaluate the prominent fluorophores as well as the hemoglobin concentration within normal and tumor brain tissues is emphasized. [DOI: 10.1117/1.JBO.18.6.067002]

Keywords: brain tumor; optical diagnosis; endogenous fluorophores; collagen; flavin adenine dinucleotide; hemoglobin; porphyrin; linear discriminant analysis.

Paper 130071RR received Feb. 6, 2013; revised manuscript received Apr. 21, 2013; accepted for publication Apr. 23, 2013; published online Jun. 3, 2013.

1 Introduction

Cancers of the brain and central nervous system (CNS) are recognized as global threats. According to the global cancer statistics, 238,000 cases of cancers of the brain and CNS have been recognized worldwide. The overall estimated mortality of 1.9%, with nearly an equal male to female ratio is caused by brain and CNS tumors.[1] The rate is higher in developed countries compared to developing or under-developed countries. The lower rate of mortality reported in the less-developed countries may be due to the lack of intensive diagnostic facilities which leads to lower incidence rates being reported.[2] Genetic susceptibility, exposure to ionizing radiation, dietary intake, lifestyle factors, family history, and immune factors are proposed as the main etiological factors.[3] As the brain is the most sensitive organ in the human body, brain tumor patients require intensive medical care. The cost for brain tumor prognosis is nearly 25% of the entire annual cost of the care for overall cancer patients.[4]

Excision biopsy followed by histopathology is the widely accepted gold standard for tumor screening. But this technique is time consuming and restricted to limited statistical confidence level due to operator variability.[5] Minimally invasive and *ex vivo* optical spectroscopic techniques based on fluorescence and absorbance of tissues such as fluorescence, diffuse reflectance, infrared, and Raman spectroscopy are the emerging tools in tumor diagnosis. These techniques give promising results in tumor differentiation.[6–10]

Fluorescence and diffuse reflectance spectroscopic techniques are cost effective compared with other spectroscopic techniques, and hence affordable to financially needy patients. Early diagnosis and even minute variations in the biochemistry of the tissue can be easily detected with these techniques. Analysis of the fluorescence peaks corresponding to major fluorophores can be utilized for the effective monitoring of biochemical changes in the tissue.[8–13] These fluorophores include collagen, nicotinamide adenine dinucleotide (NADH), flavin adenine dinucleotide (FAD), phospholipids, and porphyrin. Additionally, the use of diffuse reflectance spectroscopy can monitor the variation in hemoglobin, which is an absorber within the tissue.[11,14–18]

For many years, application of fluorescence spectroscopy has become an area of interest among many clinical and oncologic research groups. These studies demonstrate the variations in endogenous fluorophores of malignant and normal tissues using *in vivo* and *ex vivo* fluorescence spectroscopy.[9–11] But studies relating the fluorescence behavior of the fluorophores of brain tumor tissues are limited.[12,19] Available reports are on the fluorescence study of 5-aminolevunic acid (ALA) induced protoporphyrin synthesis in the brain tumor.[20,21] These studies

Address all correspondence to: Ramapurath S. Jayasree, Sree Chitra Tirunal Institute for Medical Sciences and Technology, Biophotonics and Imaging Lab, Biomedical Technology Wing, Poojappura, Thiruvananthapuram, Kerala, India 695 012. Tel: +91 4712520273 (O)/9495948221 (M); Fax: +91 471 2341814; E-mail: jayashreemenon@gmail.com

0091-3286/2013/$25.00 © 2013 SPIE

are inadequate for judging the exact biochemical alterations that occur in brain tissues during malignant transformation.

Hemoglobin is a nonfluorescent metalloprotein.[22,23] Hemoglobin peak in the autofluorescence spectra of tissues has been considered as an anomaly by a majority of the researchers.[8,11,24,25] In order to correct these artifacts in fluorescence spectra due to blood absorption, many research groups have adopted mathematical correction factors assisted by the results of diffuse reflectance spectroscopic data.[11,25,26] Mallia et al. and de Veld et al. have reported a first-order approximation method that involves division of fluorescence spectral data with the diffuse reflectance data from the same tissue site to remove the hemoglobin absorption artifacts.[11,25] Thus, the possibilities of using fluorescence spectroscopy for evaluating the changes in the hemoglobin concentration have not been exploited in detail. In 2009, Liu and Vo-Dinh proposed a ratio-metric method based on spectral filtering modulation (SFM) for the estimation of total hemoglobin and oxygen saturation using synthetic tissue phantom models.[27] However, this has not been demonstrated experimentally on human tissue so far. In the present study, we have taken up this theory and tried to apply it practically and propose to evaluate the total hemoglobin concentration in brain tumor lesions. In addition, we also propose to evaluate the biochemical changes of prominent endogenous fluorophores such as collagen, FAD, phospholipids, and porphyrin within the brain tissue. For this, we have analyzed adjacent normal and tumor tissues from patients with intra-axial tumors like astrocytoma and glioma and extra-axial tumors like meningioma and schwannoma. The exact differentiation of the tumor and adjacent normal tissue among different groups was evaluated using linear

Table 1 Clinical report of the patients involved in this study.

Tumor type	Sl. No.	Sex	Age	Number of tissue studied		Histopathological grading	WHO grade
				Adjacent normal	Tumor		
Astrocytoma	1	F	36	2	1	Mixed oligoastrocytoma	II
	2	M	32	1	2	Oligodendroglioma	II
	3	F	15	1	1	Pilocytic astrocytoma	I
	4	M	14	3	1	Mixed astrocytoma	II
	5	M	32	1	2	Ependymoma	II
	6	M	17	2	1	Pilocytic astrocytoma	I
	7	F	29	1	1	Subependymoma	I
	8	M	34	1	2	Mixed astrocytoma	II
	9	M	14	2	1	Pilocytic astrocytoma	I
	10	F	47	1	2	Mixed oligoastrocytoma	II
	11	F	38	3	1	Oligodendroglioma	II
	12	M	29	2	1	Mixed oligoastrocytoma	I
Glioma	1	M	56	2	1	Glioblastoma multiforme	IV
	2	M	42	1	0	Anaplastic astrocytoma	III
	3	M	38	1	2	Anaplastic oligodendroglioma	III
	4	M	35	2	1	Glioblastoma multiforme	IV
	5	M	33	1	1	Anaplastic astrocytoma	III
	6	F	32	1	1	Anaplastic oligodendroglioma	III
	7	M	32	2	1	Glioblastoma multiforme	IV
	8	M	25	2	1	Glioblastoma multiforme	IV
	9	F	59	1	1	Anaplastic oligodendroglioma	III
	10	M	61	2	1	Glioblastoma multiforme	IV

Table 1 (*Continued*).

Tumor type	Sl. No.	Sex	Age	Number of tissue studied		Histopathological grading	WHO grade
				Adjacent normal	Tumor		
Meningioma	1	M	62	1	1	Fibroblastic meningioma	I
	2	F	41	2	1	Atypical meningioma	II
	3	F	44	2	1	Meningothelial meningioma	I
	4	F	47	1	0	Anaplastic meningioma	III
	5	F	55	3	1	Mixed meningioma	I
	6	F	44	1	1	Meningothelial meningioma	I
	7	M	58	1	1	Atypical meningioma	II
	8	M	60	1	1	Fibroblastic meningioma	I
	9	F	42	2	1	Atypical meningioma	II
	10	F	46	2	1	Mixed meningioma	I
	11	M	54	2	0	Anaplastic meningioma	III
	12	M	62	1	1	Atypical meningioma	II
	13	M	42	2	1	Meningothelial meningioma	I
	14	F	48	2	1	Anaplastic meningioma	III
Schwannoma	1	F	41	2	1	Schwannoma	I
	2	F	65	1	2	Schwannoma	III
	3	F	38	1	1	Schwannoma	II
	4	M	34	1	1	Schwannoma	I
	5	M	36	1	0	Schwannoma	I
	6	F	17	1	1	Schwannoma	II
	7	M	22	2	1	Schwannoma	II
	8	M	39	1	1	Schwannoma	I
	9	F	57	1	1	Schwannoma	II
	10	F	31	1	1	Schwannoma	I

discriminant analysis (LDA). Here, we report the efficacy of autofluorescence spectroscopy to serve as a single entity to discriminate tumor tissues from normal ones by analyzing the variations in both endogenous fluorophores and chromophores involved.

2 Materials and Methods

2.1 *Study Population and Sample Collection*

Tissue samples were collected from the patients who underwent surgery at the Department of Neurosurgery, Sree Chitra Tirunal Institute for Medical Science and Technology, Thiruvananthapuram. All spectral acquisitions were done within 1 h of surgery. These samples were cut into small pieces of 2- to 3-mm thickness with a cross-sectional dimension of ~10× 10 mm. After spectroscopic acquisition, these tissue samples were processed for pathological evaluation. Tissues were pathologically evaluated in duplicate and graded as normal or tumor. The uninvolved portion of the surgically removed tumor samples, which were termed as normal by pathological report, is referred to as adjacent normal throughout this study. As per the evaluation by the pathologist, the spectra of tumor and adjacent normal-appearing brain tissues were classified into four groups as astrocytoma, glioma, meningioma, and schwannoma. Intra-axial tumors like astrocytoma and glioma which included in this study are excised from the white matter area of brain. Extra-axial tumors like meningioma are excised from dura mater, and schwannoma from cranial nerves associated with Schwann cells. Patient details and

pathological report of the surgically excised tumor tissue are given in Table 1.

2.2 *Instrumental Setup*

The autofluorescence measurements were carried out using the Spectrofluorometer Fluorolog-III (Jobin Yvon Inc., Edison, New Jersey). Spectroscopic parameters such as slit width, optimum integration time, and spectral range were kept constant for all samples. The excitation source was the light from a 450 W Xenon lamp. The desired excitation wavelength was selected using monochromator, and the light rays were allowed to fall perpendicular to the tissue surface with a spot size of 2×6 mm. The emission from the sample was collected at an angle of 22.5 deg with respect to the excitation beam using photomultiplier tube. The excitation wavelengths of 320 and 410 nm were selected using Datamax™ software (Datamax, Round Rock, Texas) and the inbuilt double-grating monochromator. Emission spectra in the range of 350 to 600 and 440 to 750 nm were recorded for 320 and 410 nm excitations, respectively.

2.3 *Data Processing and Analysis*

2.3.1 *Processing of spectra*

All spectra were baseline corrected and then normalized with respect to the maximum intensity of the peaks at 460 ± 10 and 500 ± 10 nm for the 320 and 410 nm excitations, respectively. From the normalized data, peak intensity corresponding to the major peaks was extracted. Using SPSS-17 (SPSS Inc., Chicago, Illinois), one way analysis of variance (ANOVA) was carried out for checking the variations in the prominent fluorescence peak intensity between the adjacent normal and tumor tissues.

2.3.2 *Total hemoglobin concentration estimation*

Schematic representation of SFM effect on autofluorescence spectra due to hemoglobin absorption from brain tumor tissues is given in Fig. 1. The total hemoglobin concentration was determined by considering the ratio of fluorescence emission intensities at 500 and 570 nm of the 410 nm excited spectra. The extinction coefficients of oxygenated and deoxygenated hemoglobin at these wavelengths are equal. Hence the ratio between these provides the total concentration of hemoglobin. The calculations were done using the following equations as per the method given by Liu and Vo-Dinh.[27]

$$\text{Total hemoglobin concentration} = \text{FI}_{500}/\text{FI}_{570}.$$

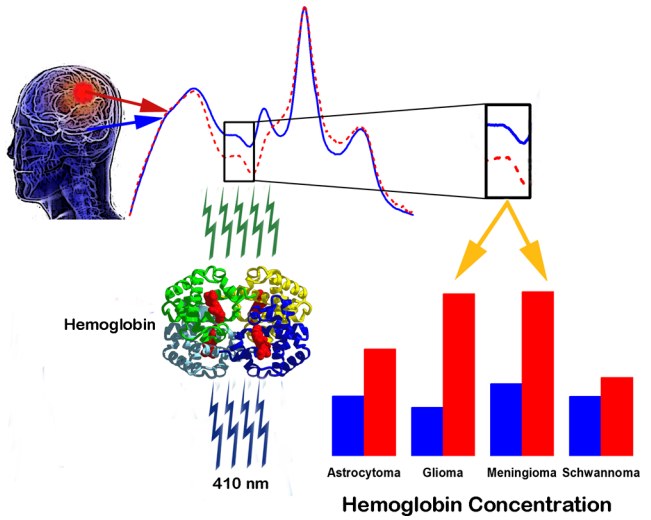

Fig. 1 Schematic representation of spectral filtering modulation (SFM) effect on autofluorescence spectra due to hemoglobin absorption in brain tissue.

2.3.3 *Multivariate analysis*

LDA is a classical multivariate statistical analysis approach for dimensionality reduction. It computes an optimal projection by minimizing the "within-class distance" and maximizing the "between-class distance" simultaneously achieving maximum class discrimination. In this study, we performed LDA on normalized spectra in the range of 350 to 600 nm and 440 to 750 nm for 320 and 410 nm excitations, respectively, using SPSS. Discriminant analysis was carried out on the normalized datasets which transformed the scores into a single discriminant score. The classification based on "leave one out" method of cross-validation produces a confusion matrix that compares predicted versus actual group membership. This classification result was used to calculate sensitivity and specificity as per previously reported methods.[13,28]

3 Results

3.1 *Fluorescence Spectral Features*

Autofluorescence spectra at two different excitation wavelengths, 320 and 410 nm, were collected and considered for the study. Broad peaks around 380, 460, and 560 nm were observed for the 320-nm excited spectra. Spectra corresponding to this excitation are given in Fig. 2. At 410-nm excitation, five distinct peaks around 500, 560, 590, 630, and 695 nm were observed for all the samples (Fig. 3). A marked difference in the fluorescence peaks were observed between tumor and adjacent normal tissue for both excitations. In both excitations the spectra were normalized with respect to the peaks at 460 and 500 nm, respectively, and hence these peaks are not considered for the analysis.

3.1.1 *Spectral features of 320 nm excited spectra*

An intense peak at 380 nm is observed for both astrocytoma and glioma. A shoulder around 510 nm for the peak at 460 nm and a weak peak around 560 nm are also observed for these tumors. A similar pattern is observed for the adjacent normal tissue also. But the peak around 380 nm is more intense, whereas the peak around 510 nm is less intense compared to the tumor tissue. The 560 nm peak is more prominent in the case of tumor tissue compared to the adjacent normal. For glioma, the peak around 380 nm is weak for the tumor tissue compared to the adjacent normal. The shoulder at 510 nm is not well resolved for the tumor tissue compared to that of adjacent normal. But the peak around 560 nm appears to be more resolved than the normal tissues.

An entirely different spectral pattern is observed for extra-axial tumor tissues. For meningioma and corresponding adjacent normal tissues at 320-nm excitation, the peak around 380 nm is many fold more intense than the other peaks. For

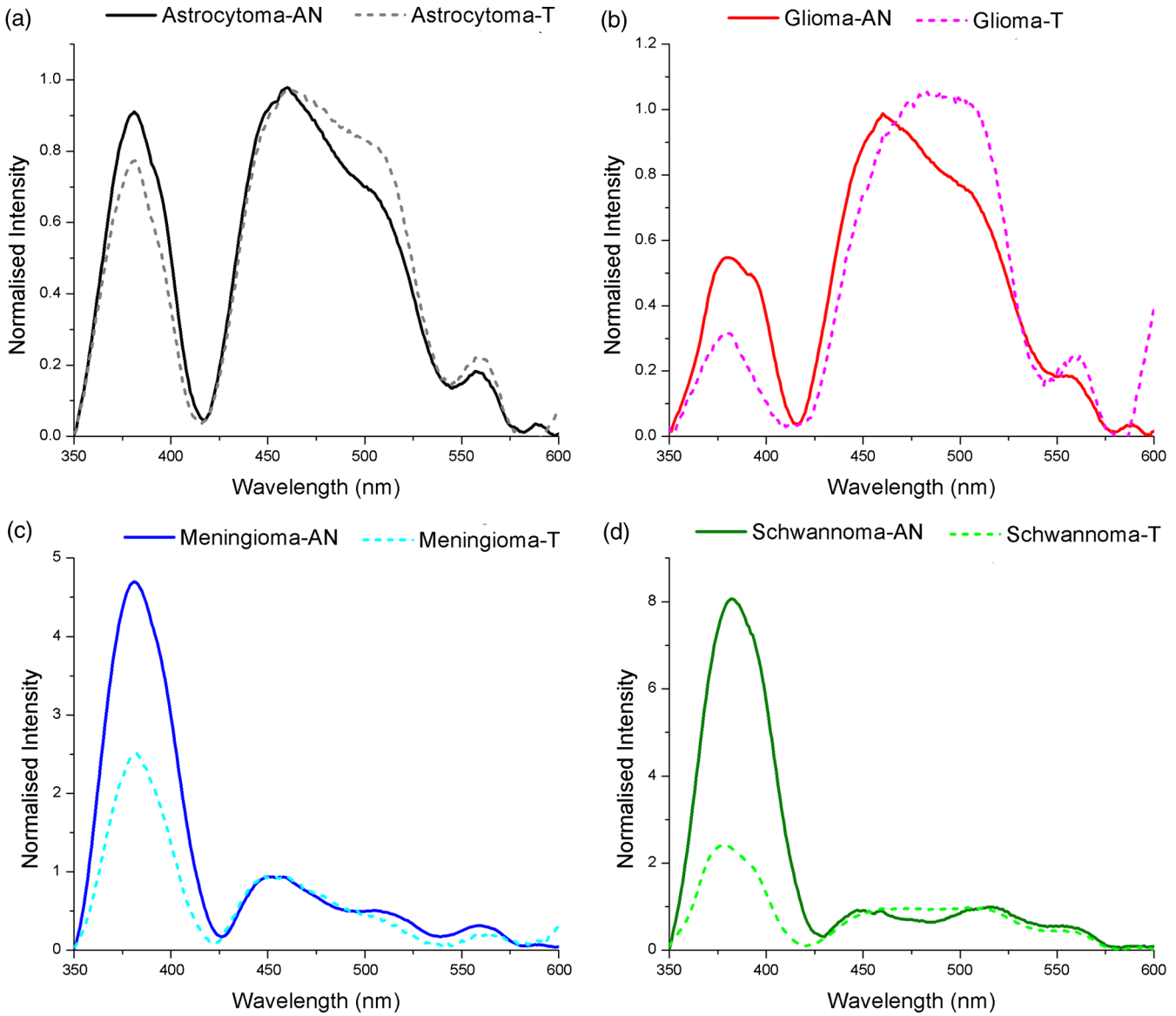

Fig. 2 Averaged fluorescence emission spectra of adjacent normal and tumor samples of (a) astrocytoma, (b) glioma, (c) meningioma, and (d) schwannoma at 320 nm excitation.

the tumor tissue, this peak is considerably weaker compared to that of normal tissue. The peak around 510 nm is absent, and the peak at 560 nm is very weak for the tumor tissues, whereas well-resolved peaks are observed around 510 and 560 nm for the adjacent normal tissue. Similar to meningioma, spectra of schwannoma also have the most intense peak around 380 nm. Here also, this peak is much weaker in tumor compared to normal tissues. Well-resolved peaks are observed around 510 and 560 nm for adjacent normal compared to the tumor tissues.

ANOVA was performed on the maximum peak intensity values and the results are given in Table 2. A significant difference ($p < 0.05$) in the intensity is observed for 380 nm peak of glioma and adjacent normal. But in the case of astrocytoma ($p = 0.142$), meningioma ($p = 0.085$), and schwannoma ($p = 0.120$) intensity difference for this peak is not significant. Differences among other peaks of 320 nm excited spectra are also found to be insignificant.

3.1.2 *Spectral features of 410 nm excited spectra*

Here, adjacent normal tissue showed well-defined peaks when compared to the tumor tissue in all the four cases. A varied intensity pattern is observed for the different peaks among different tissues. Considering the peak around 500 nm, a blue shift is observed in the case of tumor tissue compared to the normal. This is true for all the tumor types considered. When the whole spectrum is analyzed, the spectral intensity around 560 and 590 nm is much less compared to corresponding adjacent normal tissues. For astrocytoma and glioma, the peak around 560 nm is more prominent whereas it is not resolved for meningioma and schwannoma. Well-defined highly resolved peaks are observed around 590 nm for all the adjacent normal tissues. Interestingly, this peak disappears from the tumor spectra. The peaks at 630 and 695 nm are of nearly equal intensity for both adjacent normal and tumor tissues in all cases. But a significant difference in peak intensity is observed for these peaks among different tumor types considered

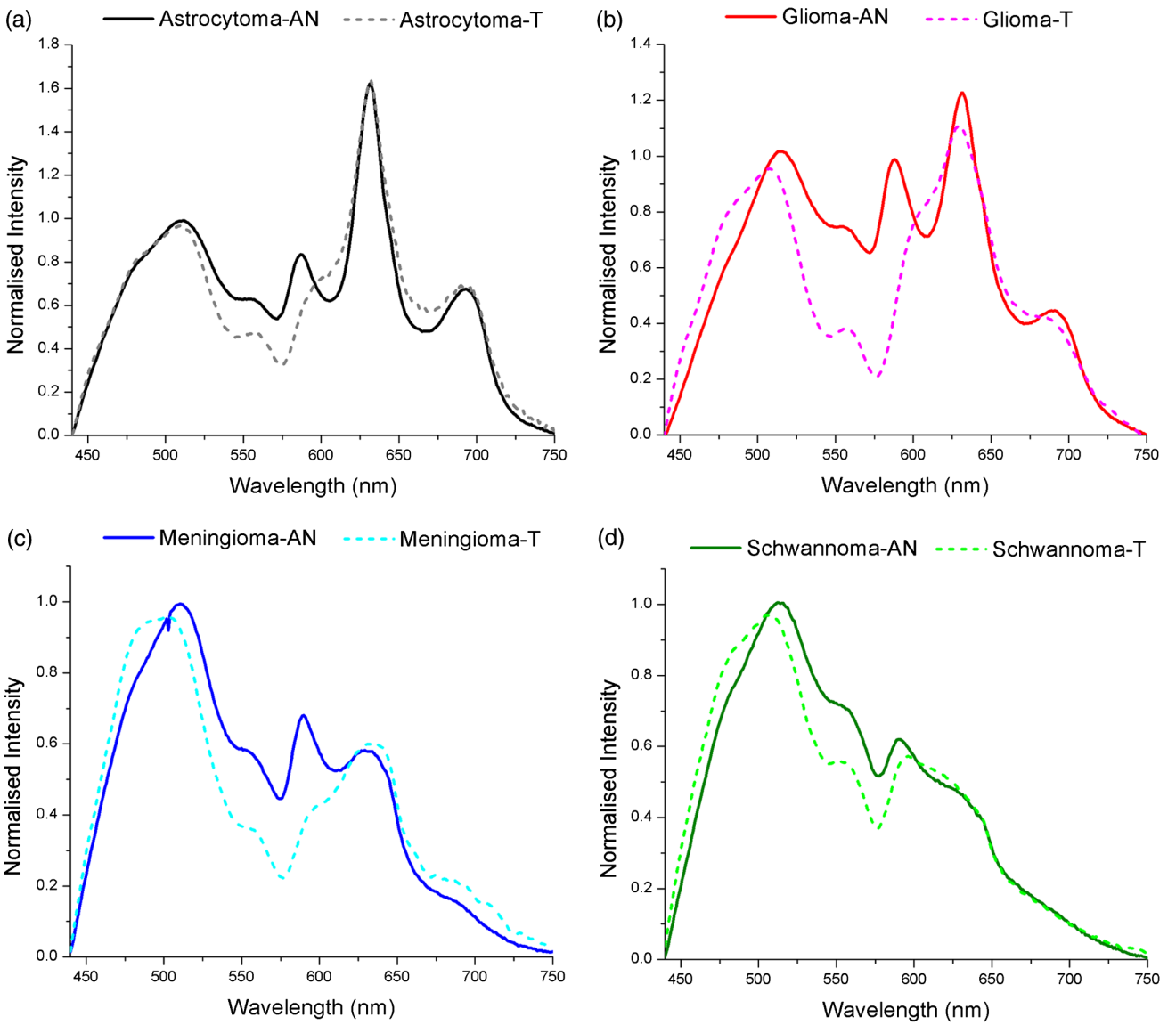

Fig. 3 Averaged fluorescence emission spectra of adjacent normal and tumor samples of (a) astrocytoma, (b) glioma, (c) meningioma, and (d) schwannoma at 410 nm excitation.

(Fig. 3). For extra-axial brain tumors and its adjacent normal tissues, the peak at 695 nm is not resolved and appears as a valley whereas characteristic medium intense and well-resolved peaks are observed in intra-axial brain tissues.

ANOVA gives a significant difference in the peak intensity ($p < 0.05$) for all the four tumor types when the peak centered at 560 nm is considered. The 590 nm peak shows significant difference in the peak intensity for astrocytoma ($p = 0.023$) and glioma ($p = 0.000$), but not for meningioma ($p = 0.057$) and schwannoma ($p = 0.069$). The intensity variation of the peaks at 630 and 695 nm was also found to be insignificant among the four types of tumor.

Table 2 One way analysis of variance (ANOVA) on comparison of intensity values between adjacent normal and tumor ($p < 0.05$ are given in bold letters).

	320 nm excitation			410 nm excitation			
Tumor type	380	510	560	560	590	630	695
Astrocytoma	0.142	0.543	0.125	**0.000**	**0.023**	0.979	0.964
Glioma	**0.001**	0.895	0.122	**0.000**	**0.000**	0.786	0.720
Meningioma	0.085	0.165	0.343	**0.002**	0.057	0.893	0.281
Schwannoma	0.120	0.997	0.656	**0.024**	0.069	0.273	0.534

3.2 *Total Hemoglobin Estimation*

Total concentration of hemoglobin values calculated for astrocytoma, glioma, meningioma, schwannoma, and the corresponding adjacent normal tissues are given in Fig. 4. It is clear that there is considerable increase in the total hemoglobin concentration for all tumor tissues compared to the normal ones. This increase is found to be statistically significant ($p < 0.005$) irrespective of the tumor type.

3.3 *Linear Discriminant Analysis for Tissue Classification*

The pairwise discrimination score for astrocytoma, glioma, meningioma, schwannoma, and corresponding adjacent normal tissues are given in Figs. 5 and 6. From these plots, it is clear that the intergroup distance for tumor and adjacent normal is very well separated among the various groups. It is noted that the intergroup distance between the glioma and adjacent normal is highly significant compared to astrocytoma, meningioma, and schwannoma. This is more prominent in the case of data based on the 410 nm excitation. A discrimination line drawn at 0 gives a good differentiation. In the case of 320 nm excited spectra, the discrimination score for tumor is observed considerably above the discrimination line, and for adjacent normal it is below the discrimination line. But for the 410 nm excitation, the pairwise discrimination score for tumor is considerably below the discrimination line, and for adjacent normal tissue it is considerably above. Using the position of pairwise discrimination scores, the number of true positive and negative values as well as the number of false positive and negative values was obtained. Results from this binary classification are utilized for the discrimination of tissues (Table 3).

4 Discussions

In this study, we have attempted to differentiate tumor and adjacent normal brain tissue based on the changes observed in the autofluorescence spectra. We have also utilized diagnostic algorithms to interpret the wealth of spectral information for the exact differentiation of brain tumor tissues from normal. Preprocessing methods like baseline correction and normalization are also done in all cases to get better efficiency in the classification. The importance of preprocessing of spectral data has been reported earlier.[13] We have adopted the method of normalization with respect to specific peak intensity which gives better results in classification. Hence, the relative concentration of fluorophores is considered throughout this study. An excitation wavelength of 320 nm is ideal for picking up the fluorophores collagen, NADH, and FAD whose emissions are expected around 380, 460, and 510 nm, respectively. Excitation at 410 nm gives the emission values of FAD and phospholipids around 500 and 590 nm, respectively. This excitation also gives the emission of porphyrin around 630 and 695 nm.[8–13] The fluorescence peaks of this study are assigned accordingly.

Variation of collagen in tumor, especially in brain tumor, is a hot area of discussion.[6] In the present study, the collagen level as observed by the peak around 380 nm is less intense for tumor tissues than the normal one in all the cases. Also among the four tumor types considered, extra-axial tumors and its adjacent normal show a high level of collagen compared to intra-axial tumor tissues. The reason for this is intra-axial brain tissues have only 20% of extracellular matrix (ECM) compared to its total volume, whereas extra-axial brain tissues roughly have a balance

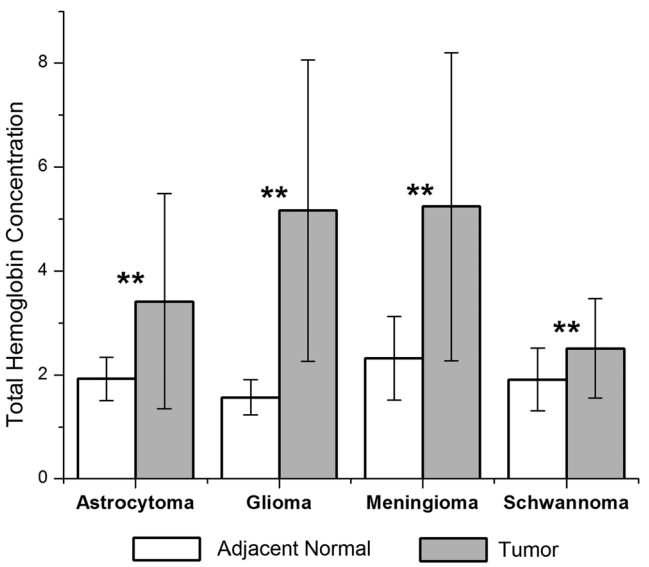

Fig. 4 Total hemoglobin concentration of adjacent normal and tumor tissue. Data shown are in the form mean + SD. Significance (**$p < 0.005$) of differences between adjacent normal and tumor tissues.

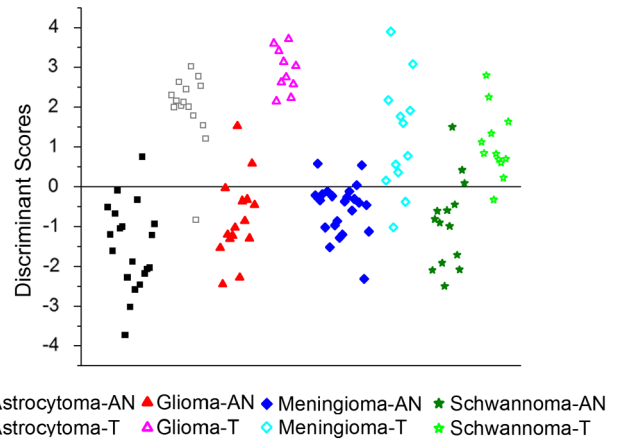

Fig. 5 Pairwise discriminant plot based on linear discriminant analysis (LDA) for adjacent normal and tumor samples for 320 nm excitation.

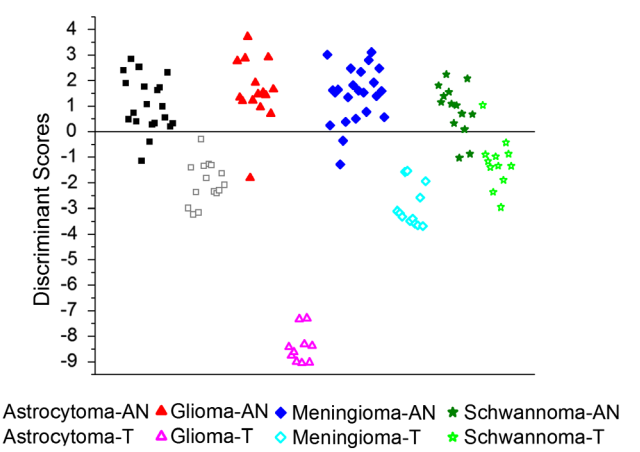

Fig. 6 Pairwise discriminant plot based on LDA for adjacent normal and tumor samples for 410 nm excitation.

Table 3 Classification efficacy obtained using linear discriminant analysis (LDA) for the differentiation of tumor and adjacent normal tissues.

	320 nm excitation		410 nm excitation	
Tumor type	Sensitivity (%)	Specificity (%)	Sensitivity (%)	Specificity (%)
Astrocytoma	93.33	95	93.33	95
Glioma	100	93.33	100	93.33
Meningioma	83.33	91.31	100	91.31
Schwannoma	91.67	78.57	91.67	92.86

of 50% to 50% between ECM and cells.[29] When the collagen level between the tumor and adjacent normal is considered, a decrease in collagen level is observed in all the four types. Using protein secondary structure determination of infrared spectra, Noreen et al. have observed that the level of fibrillar collagen (collagen I, III, and V) decreases and nonfibrillar collagen (collagen IV and VI) increases in brain tumor compared to healthy tissues.[6]

The decrease in collagen level may be due to the degradation of ECM which occurs during tumor cell invasion process to facilitate migration of neoplastic cells to the surrounding tissues.[30,31] Specifically in the case of brain tumors, overexpression of matrix metalloproteinase enzyme will degrade fibrillar and nonfibrillar collagens leading to the degradation of ECM.[32] Due to the changes in the ECM protein components, tumor angiogenesis and tumor cell proliferation and invasion occur in brain.[30,31,33] The current findings lead to the conclusion that total collagen level in brain decreases as tissue transforms from normal to tumor.

In the 410 nm excited spectra, the phospholipid peak at 590 nm is less intense for tumor tissue than for the normal, indicating a decrease in the lipid level in the tumor tissue. A reduction in the total lipid level in brain tumor has been reported earlier by Köhler et al.[34] A possible reason for this can be lipid peroxidation that occurs in brain tumor as a result of the decrease in antioxidant enzymes such as catalase, superoxide dismutase, and glutathione reductase.[35,36] Decrease in such antioxidant enzymes induces oxidative stress in brain tissues and results in lipid peroxidation.

The fluorescence peaks of porphyrin are observed around 630 and 695 nm in the 410 nm excited spectra. In this study, the level of porphyrin is found to be highest for astrocytoma, followed by glioma, meningioma, and schwannoma. A similar pattern is observed for the normal tissues as well. These peaks are very weak and not resolved in the case of extra-axial tissues compared to intra-axial tissues.

Comparison of Fig. 3(a) and 3(b) to that of 3(c) and 3(d), it is clear that the level of porphyrin is less in extra-axial tissues compared to intra-axial tissues. It is also seen that the porphyrin level does not vary much between the tumor and normal tissue, irrespective of the tissue types. But an increase in porphyrin level in brain tumor has been reported in ALA-induced fluorescence method. This is due to the fact that ALA gets converted to proptoporphyrin by the ferro chelates present in the tumor.[20,21] No other reports are available on the level of porphyrin in brain tumors.

For biological samples, the emission of FAD is expected in the 500 to 530 nm range for both excitations considered.[10–13] But in the 320-nm excited spectra, we observed a blue shift for this peak from the expected value of 520 nm. The same is observed again in the 410-nm excited spectra, but only for the tumor samples. In the study using synthetic tissue phantoms, Liu and Vo-Dinh have reported a blue shift in the FAD peak on increasing the concentration of hemoglobin.[27] In the present study it is also very clear from the 410-nm excited spectra that the blue shift is noticeable in cases of higher hemoglobin concentration (Fig. 3). So, we ascribe the observed shift as due to the increase in hemoglobin concentration in the tumor tissue.

The peak appearing at 560 nm is assigned to the hemoglobin absorption. So far, this peak has not been considered seriously by any research groups for differentiating tissue biochemistry. Many research groups have reported this peak as an anomaly.[8,11,24,25] But, Liu and Vo-Dinh, using synthetic fluorescent tissue phantoms, demonstrated that this peak can be used to estimate the total hemoglobin concentration.[27] This theory has been later demonstrated experimentally on tissue phantoms with varying FAD concentrations and glioma-induced rats.[37] In this study, it is demonstrated that the emission path length of fluorescence light is a crucial factor in the determination of total hemoglobin concentration. Emission path length of fluorescence light depends on the illumination and collection geometry of the optical probe. This path length must be long enough, so that the effect of absorption on fluorescence intensity due to hemoglobin is significant. It is also found that SFM effect on the fluorescence spectra due to hemoglobin and its variation is clearly identifiable around 560 nm when excited around 410 nm. This justifies the selection of 410 nm excitation in our present study for the estimation of total hemoglobin concentration.

In brain tumor, the total hemoglobin concentration is an index of angiogenesis.[38,39] To date, no reports are available on the evaluation of total hemoglobin concentration of different types of brain tumor lesions using fluorescence spectroscopy. Using diffuse reflectance spectroscopy studied *ex vivo* and *in vivo*, various groups have reported that total hemoglobin concentration increases when the tissue becomes malignant.[40,41] Our results on SFM effect on the fluorescence spectra due to hemoglobin absorption show significant increase in hemoglobin concentration in the tumor tissue which is in agreement with these findings. From the observations, we suggest that fluorescence spectroscopy is an ideal tool for the effective quantification of total hemoglobin concentration within brain tissue.

Although the explained method is promising, we envisage some limitations that would have affected the results of the study due to certain factors which need to be discussed. As is seen from Fig. 4 where hemoglobin concentration is demonstrated, the error bars appears to be high. This may be because of the fact that we have considered adjacent tissue of the tumor as normal ones for the analysis, as it is impossible to have actual normal tissue of the human brain for the study. Hence, there is very high chance that the adjacent tissue considered here had pathological transformations, at least in some cases, which could be the reason for the large deviations observed in these results. Moreover, the deviations observed in hemoglobin concentration is not affecting the classification of the tissue as is evidenced by the significant difference in the ANOVA values between adjacent normal and tumor tissues.

The differentiation of normal from tumor tissue using LDA yielded a sensitivity of 83% to 100%, 93% to 100% and overall

specificity of 91% to 95%, respectively, for 320 and 410 nm excited spectra. A direct correlation between the intergroup distance between tumor and normal tissue, and the grading of the tumor is very clear from Figs. 5 and 6. Intergroup distance is maximum between glioma and adjacent normal, whereas it is minimum for schwannoma and corresponding normal. The discrimination is clearer with the dataset of 410 nm excited spectra. This further projects the efficacy of excitation wavelength around 410 nm in the evaluation of hemoglobin concentration than that of 320 nm. As by Liu and Vo-Dinh, excitation wavelength around 410 nm is the most suitable for evaluation of hemoglobin concentration than any other excitation wavelength.[17]

Previously, Butte et al. have reported an overall sensitivity of 25% to 100% and specificity of 78% to 98% to differentiate normal brain tissues, low grade glioma and high grade glioma using fluorescence lifetime spectroscopy.[42] In a study using fluorescence and diffuse reflectance spectroscopy, Lin et al. have reported an overall sensitivity and specificity of 76% to 100% to discriminate normal from brain tumor tissues.[19] Another study by Saraswathy et al. reported a sensitivity and specificity of 86% to 100% and 66% to 100% using principal component analysis in differentiating adjacent normal from brain tumor tissue.[12] In the present study, we report a better sensitivity and specificity than the previously reported ones. Moreover, we have considered not only the endogenous fluorophores but also the chromophore, hemoglobin using the single technique in achieving this discrimination. The current method provides high sensitivity and specificity compared to other studies reported earlier. These results can be considered further in the development of minimally invasive methodology based on fluorescence spectroscopy which will help to differentiate brain tumor, in the future.

5 Conclusions

Emissions from endogenous fluorophores and hemoglobin can be utilized for the effective characterization and classification of different types of brain tumors and normal tissues. Inexpensive and easy to handle techniques of autofluorescence spectroscopy can be utilized for the evaluation of both fluorophores and chromophores simultaneously. As this method can directly be used to monitor hemoglobin variation, separate equipment and measuring protocols are not required for diffuse reflectance and fluorescence measurements. The variations in the collagen and lipid levels due to the degradation of ECM and lipid peroxidation in tumor tissues can also be used to discriminate the tissue biochemistry. Additionally, data analysis methods like LDA further support the discrimination between normal and tumor tissues. A study focused on larger sample set is necessary to facilitate the use of this technique in clinical set up. Further studies in this direction are in progress, and we believe that the application of this technique in clinical practice will be a reality in the very near future.

Acknowledgments

The financial support received from the Board of Research in Nuclear Sciences, Department of Atomic Energy, Government of India is sincerely acknowledged. Shaiju S. Nazeer and Ariya Saraswathy acknowledge Council of Scientific and Industrial Research, India for the Senior Research Fellowships.

References

1. J. Ferlay et al., "Estimates of worldwide burden of cancer in 2008: GLOBOCAN 2008," *Int. J. Cancer* **127**(12), 2893–2917 (2010).
2. H. Ohgaki and P. Kleihues, "Epidemiology and etiology of gliomas," *Acta Neuropathol.* **109**(1), 93–108 (2005).
3. M. L. Bondy et al., "Brain tumor epidemiology: consensus from the Brain Tumor Epidemiology Consortium," *Cancer* **113**(7), 1953–1968 (2008).
4. R. G. Steen, *A Conspiracy of Cells: The Basic Science of Cancer*, Plenum Press, New York (1993).
5. D. C. Fernandez et al., "Infrared spectroscopic imaging for histopathologic recognition," *Nat. Biotechnol.* **23**(4), 469–474 (2005).
6. R. Noreen et al., "Detection of collagens in brain tumors based on FTIR imaging and chemometrics," *Anal. Bioanal. Chem.* **401**(3), 845–852 (2011).
7. J. L. Jayanthi et al., "Comparative evaluation of the diagnostic performance of autofluorescence and diffuse reflectance in oral cancer detection: a clinical study," *J. Biophoton.* **4**(10), 696–706 (2011).
8. D. L. Heintzelman et al., "Optimal excitation wavelengths for *in vivo* detection of oral neoplasia using fluorescence spectroscopy," *Photochem. Photobiol.* **72**(1), 103–113 (2000).
9. P. S. Haris et al., "Autofluorescence spectroscopy for the *in vivo* evaluation of oral submucous fibrosis," *Photomed. Laser Surg.* **27**(5), 757–761 (2009).
10. N. Ramanujam, "Fluorescence spectroscopy of neoplastic and non-neoplastic tissues," *Neoplasia* **2**(1–2), 89–117 (2000).
11. R. J. Mallia et al., "Clinical grading of oral mucosa by curve-fitting of corrected autofluorescence using diffuse reflectance spectra," *Head Neck* **32**(6), 763–779 (2010).
12. A. Saraswathy et al., "Optimum wavelength for the differentiation of brain tumor tissue using autofluorescence spectroscopy," *Photomed. Laser Surg.* **27**(3), 425–433 (2009).
13. S. N. Shaiju et al., "Habits with killer instincts: *in vivo* analysis on the severity of oral mucosal alterations using autofluorescence spectroscopy," *J. Biomed. Opt.* **16**(8), 087006 (2011).
14. R. Mallia et al., "Oxygenated hemoglobin diffuse reflectance ratio for *in vivo* detection of oral pre-cancer," *J. Biomed. Opt.* **13**(4), 041306 (2008).
15. N. Subhash et al., "Oral cancer detection using diffuse reflectance spectral ratio R540/R575 of oxygenated hemoglobin bands," *J. Biomed. Opt.* **11**(1), 014018 (2006).
16. N. Yadav et al., "*In vivo* detection of epileptic brain tissue using static fluorescence and diffuse reflectance spectroscopy," *J. Biomed. Opt.* **18**(2), 027006 (2013).
17. C. S. Prasanth et al., "*In vivo* inflammation mapping of periodontal disease based on diffuse reflectance spectral imaging: a clinical study," *J. Biomed. Opt.* **18**(2), 026019 (2013).
18. Z. Volynskaya et al., "Diagnosing breast cancer using diffuse reflectance spectroscopy and intrinsic fluorescence spectroscopy," *J. Biomed. Opt.* **13**(2), 024012 (2008).
19. W. C. Lin et al., "*In vivo* brain tumor demarcation using optical spectroscopy," *Photochem. Photobiol.* **73**(4), 396–402 (2001).
20. T. Ando et al., "Precise comparison of protoporphyrin IX fluorescence spectra with pathological results for brain tumor tissue identification," *Brain Tumor Pathol.* **28**(1), 43–51 (2011).
21. J. C. O. Richter et al., "Fluorescence spectroscopy measurements in ultrasonic navigated resection of malignant brain tumors," *Laser Surg. Med.* **43**(1), 8–14 (2011).
22. M. Y. Berezin and S. Achilefu, "Fluorescence lifetime measurements and biological imaging," *Chem. Rev.* **110**(5), 2641–2684 (2010).
23. B. M. Hoffman and D. H. Petering, "Coboglobins: oxygen-carrying cobalt-reconstituted hemoglobin and myoglobin," *Proc. Natl. Acad. Sci. U. S. A.* **67**(2), 637–643 (1970).
24. J. Eng, R. M. Lynch, and R. S. Balaban, "Nicotinamide adenine dinucleotide fluorescence spectroscopy and imaging of isolated cardiac myocytes," *Biophys. J.* **55**(4), 621–630 (1989).
25. D. C. de Veld et al., "Autofluorescence and diffuse reflectance spectroscopy for oral oncology," *Lasers Surg. Med.* **36**(5), 356–364 (2005).
26. R. S. Bradley and M. S. Thorniley, "A review of attenuation correction techniques for tissue fluorescence," *J. R. Soc. Interface* **3**(6), 1–13 (2006).
27. Q. Liu and T. Vo-Dinh, "Spectral filtering modulation method for estimation of hemoglobin concentration and oxygenation based on a single fluorescence emission spectrum in tissue phantoms," *Med. Phys.* **36**(10), 4819–4829 (2009).

28. S. Ji and J. Ye, "Generalized linear discriminant analysis: a unified framework and efficient model selection," *IEEE Trans. Neural Netw.* **19**(10), 1768–1782 (2008).
29. N. Urabe et al., "Basement membrane type IV collagen molecules in the choroid plexus, pia mater and capillaries in the mouse brain," *Arch. Histol. Cytol.* **65**(2), 133–143 (2002).
30. A. C. Bellail et al., "Microregional extracellular matrix heterogeneity in brain modulates glioma cell invasion," *Int. J. Biochem. Cell Biol.* **36**(6), 1046–1069 (2004).
31. J. C. Knott et al., "Stimulation of extracellular matrix components in the normal brain by invading glioma cells," *Int. J. Cancer* **75**(6), 864–872 (1998).
32. S. K. Chintala, J. C. Tonn, and J. S. Rao, "Matrix metalloproteinases and their biological function in human gliomas," *Int. J. Dev. Neurosci.* **17**(5–6), 495–502 (1999).
33. J. Zamecnik, "The extracellular space and matrix of gliomas," *Acta Neuropathol.* **110**(5), 435–442 (2005).
34. M. Kohler et al., "Characterization of lipid extracts from brain tissue and tumors using Raman spectroscopy and mass spectrometry," *Anal. Bioanal. Chem.* **393**(5), 1513–1520 (2009).
35. G. M. Rao et al., "Role of antioxidant enzymes in brain tumours," *Clin. Chim. Acta* **296**(1–2), 203–212 (2000).
36. A. Zajdel et al., "Aldehydic lipid peroxidation products in human brain astrocytomas," *J. Neuro Oncol.* **84**(2), 167–173 (2007).
37. Q. Liu et al., "Compact point-detection fluorescence spectroscopy system for quantifying intrinsic fluorescence redox ratio in brain cancer diagnostics," *J. Biomed. Opt.* **16**(3), 037004 (2011).
38. Y. Hu et al., "EFEMP1 suppresses malignant glioma growth and exerts its action within the tumor extracellular compartment," *Mol. Cancer* **10**, 123 (2011).
39. Y. H. Zhou et al., "PAX6 suppression of glioma angiogenesis and the expression of vascular endothelial growth factor A," *J. Neuro Oncol.* **96**(2), 191–200 (2010).
40. H. W. Beumer et al., "Detection of squamous cell carcinoma and corresponding biomarkers using optical spectroscopy," *Otolaryng. Head Neck* **144**(3), 390–394 (2011).
41. H. W. Wang et al., "Diffuse reflectance spectroscopy detects increased hemoglobin concentration and decreased oxygenation during colon carcinogenesis from normal to malignant tumors," *Opt. Express* **17**(4), 2805–2817 (2009).
42. P. V. Butte et al., "Fluorescence lifetime spectroscopy for guided therapy of brain tumors," *Neuroimage* **54**, S125–S135 (2011).